JOURNAL OF GEOPHYSICAL RESEARCH, VOL. 102, NO. D12, PAGES 13,793-13,800, JUNE 27, 1997

An abrupt spring air temperature rise over the Greenland ice cap

Jeffrey C. Rogers,[1] Robert A. Hellstrom,[2] Ellen Mosley-Thompson,[1] and Chung-Chieh Wang[2]

Abstract. We report on an abrupt springtime temperature rise (ASTR) occurring over the Greenland ice cap. The abrupt 12°-15°C temperature rise typically occurs in May over a 24-36 hour period and is accompanied by a 16-22 hPa pressure rise that begins 2-3 days earlier. The Greenland ASTR is examined using composites of pressure and temperature data from Automatic Weather Stations at "Cathy" and "Kenton" for the years 1987 through 1990 and 1992 and 1993. Comparative analysis of the ASTR at coastal weather stations is made and contemporaneous atmospheric circulation variations are examined with gridded hemispheric sea level pressure and 500 hPa data. At the ice cap summit the ASTR is accompanied by an average 360 m rise in 500 hPa geopotential heights, strong surface winds, and high relative humidities. During an ASTR, concomitant air temperatures along the western coast of Greenland and on Baffin Island also rise, but with a magnitude only half that at the ice cap summit. The contemporaneous ASTR pressure rise at coastal stations is of equivalent magnitude to that at the summit and is most prominent at Greenland stations and on Iceland. Evidence is presented that the ASTR is linked to a seasonal readjustment in the regional Atlantic atmospheric circulation in which the westerlies become weakest in May and migrate northward into the Arctic. A meridional flow regime is established with southwesterly flow advecting mild air over Greenland. Blocking highs form over the Atlantic and the surface mean Icelandic low is weak, or replaced by mean high pressure. The nature and timing of the ASTR is important for planning field activities on the Greenland ice sheet. Further study of the ASTR should lead to a better understanding of boundary layer processes over the ice sheet.

Introduction

This paper reports on an abrupt springtime rise in air temperatures measured by Automatic Weather Stations (AWS) near the summit of the Greenland ice cap. The abrupt air temperature rise of 12°-15°C occurs over a 24-36 hour period during May, after which air temperatures generally remain near summer levels into August. The sudden onset of summer temperature accompanies a large rise in ice cap station air pressure that occurs over several days. The meteorological characteristics associated with the abrupt springtime temperature rise (hereinafter referred to as "ASTR") on the ice cap are described and placed within the context of larger-scale seasonal atmospheric circulation changes and regional weather variability at coastal weather stations. The potential paleoclimatological implications of the ASTR and its significance for field work on Greenland are also discussed.

The ASTR was first identified by *Stearns and Weidner* [1991a, Figure 3] who noted the sharp temperature rise in the AWS data of early May 1990. *Hellstrom* [1995] provides an extensive description of ASTR events from 1987 to 1993, including a discussion of boundary layer climatological implications of the phenomenon. The abrupt spring rise in temperature on the ice cap is also detected using satellite passive microwave brightness temperatures [Shuman *et al.*, 1995a], although the temperature response is somewhat smaller than that observed by the AWS.

Data and Methods of Analysis

AWS provide a valuable source of hourly and daily weather observations [*Bromwich and Stearns*, 1993] from remote locations where daily meteorological data are not otherwise available. The ASTR events are identified and described using 3 hourly AWS pressure and air temperature data obtained from one comparatively long-term station on the ice cap. AWS "Cathy" (72.30°N, 38.00°W) was installed by the Department of Meteorology at the University of Wisconsin [*Stearns and Weidner*, 1991b] and operated from May 1987 to June 1989. "Cathy" was subsequently moved west (72.28°N, 38.80°W) and renamed AWS "Kenton" (Figure 1). Data from the two stations were available through June 1993, at 3 hour intervals, except for a gap of missing data from January to July 1991 that precluded further analysis of the ASTR for that year. The recent 1994 data have been incorporated partially into the discussion in this paper.

Daily synoptic surface air temperature and sea level pressure observations for 11 coastal stations on Greenland, Iceland, and Baffin Island (Figure 1) are also used. These data were obtained from station models on published 12 hourly (0000 and 1200 UT) National Meteorological Center analyses, available on microfilm from the National Climatic Data Center. Daily sea level pressure and 500 hPa geopotential height analyses, available at 12 hour intervals on a hemispheric 5° x 5° latitude/longitude grid, are used for the atmospheric circulation analysis.

To examine the ASTR phenomenon, composites of the meteorological and atmospheric circulation data were produced using the superposed epoch approach. This approach produces composites, or averages, for the data set, smoothing the impact of events in individual and "unusual" years. Some discussion of unusual events contributing to the averages is provided here, but details of individual ASTR events are given by *Hellstrom* [1995]. Producing the averages, or composites, for specific time intervals before and after the event required precise timing of the ASTR in the annual AWS records. Each ASTR was identified by (1) an abrupt rise in AWS air temperatures (Figure 2) to near the summer daytime maximum temperature (approximately -10°C), (2) an accompanying and continued period of rising pressure, and (3) subsequent maintenance of higher temperatures and pressures for much of the summer. The AWS data were available every three hours, but all other data were available only twice daily. Thus, although the maximum temperature on the day of the ASTR generally occurred at 1800 UT, the ASTR date were assigned to 0000 UT of the following day, which is called "day zero" or T=0. All of the ASTR events are aligned on T=0 to form the composites.

[1]Department of Geography and Byrd Polar Research Center, Ohio State University, Columbus.

[2]Atmospheric Science Program and Byrd Polar Research Center, Ohio State University, Columbus.

Paper number 96JD03097.
0148-0227/97/96JD-03097$09.00

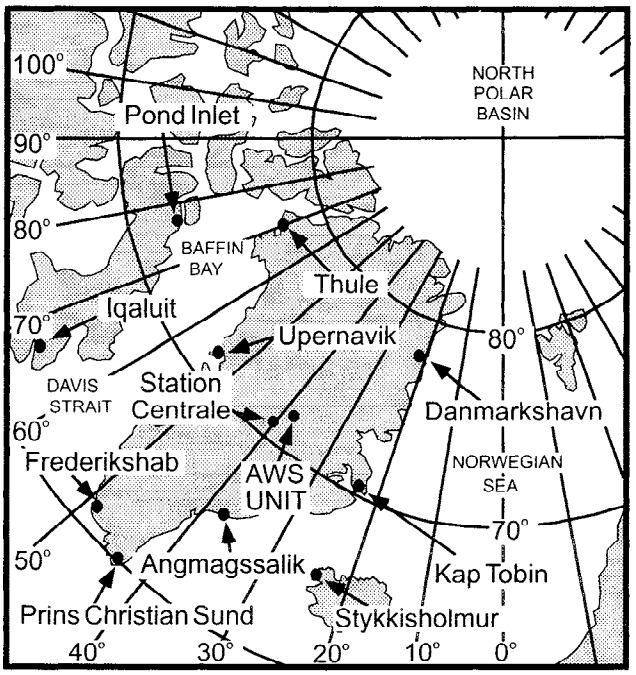

Figure 1. Location of Automatic Weather Station (AWS) "Cathy/Kenton" on the Greenland ice cap and location of coastal weather stations used in analysis of the spatial extent of the ASTR.

Meteorological Characteristics of ASTR Events

The occurrences of the ASTR (Figure 3) range from May 4 (in 1990) to May 30 (in 1989). Although the 1991 ASTR date was identified using data from AWS Klinck (72.31°N, 40.48°W), it is not included in the analysis because of an a priori decision to use only data associated with the longest record at the Cathy/Kenton site. Subsequently, *Shuman et al.* [1995b] merged data from several AWS to produce a continuous record from 1987 to mid-1991.

Figure 2 illustrates the daily composite mean maxima and minima temperatures and the daily average pressure from 15 days prior to the ASTR to 30 days after the event. The tendency for maximum temperatures to remain near -10°C for the 30 days following T=0 is evident, and the temperatures remain at this summer level into August. The daily minimum temperatures average about -22°C for the 30 post-ASTR days, approximately the same value as the average daily maximum air temperature prior to ASTR (Figure 2). Prior to the ASTR daily minima average about -37°C.

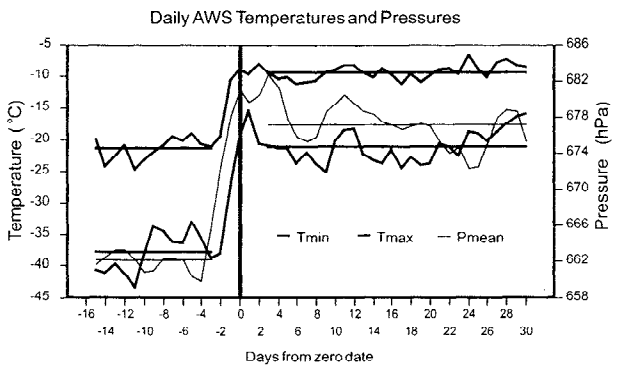

Figure 2. A 6 year composite of AWS Cathy/Kenton daily mean maximum and mean minimum air temperatures and daily mean station pressures (hPa) for the period 15 days before and 30 days after the abrupt springtime temperature rise (ASTR).

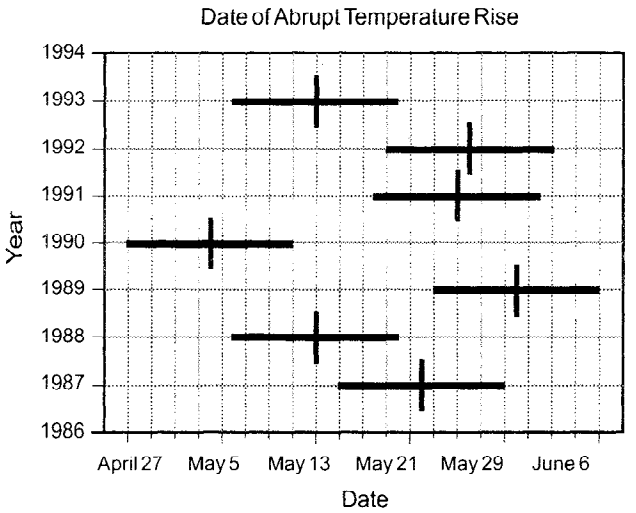

Figure 3. Dates (short vertical line) of the abrupt springtime air temperature rise occurring on the Greenland ice cap. The long horizontal bar delineates seven days prior to and seven days after the event.

The 6 year composites of the 3 hourly AWS air temperatures and station pressures (Figure 4), for seven days prior to and for seven days after the ASTR events, reveal the diurnal temperature variability. Note that the composite diurnal range of air temperatures is largest prior to the ASTR, and smallest on T=0 and T+1 after the ASTR (Figure 4). Daily minimum air temperatures average about -35°C in the preceding week and are roughly -20°C after T+1 (Figure 4). On the day prior to the ASTR the composite minimum temperature only falls to about -25°C and is followed by a dramatic warming (Figure 4). Daily maximum temperatures are about 12°C higher after T=0 and daily minima are about 15°C higher. The diurnal temperature range is reduced from 13°C (-35°C and -22°C) to 10°C (-20°C and -10°C)

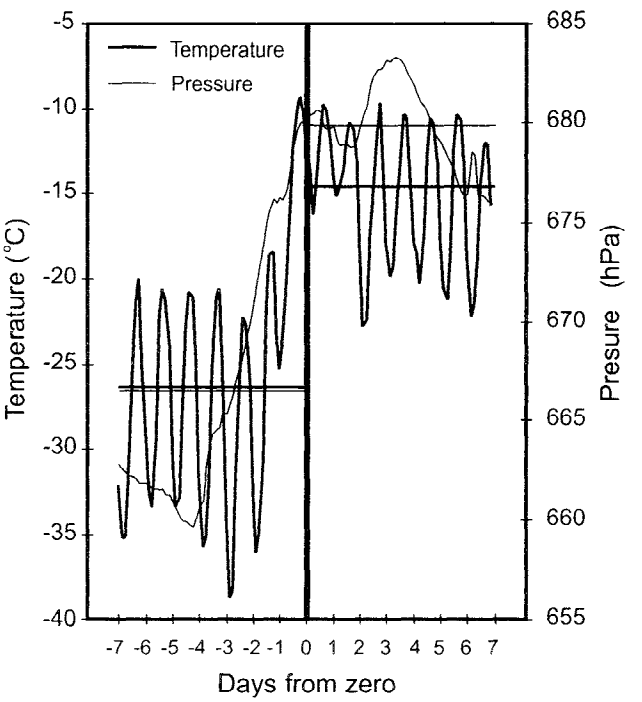

Figure 4. A 6 year composite of AWS Cathy/Kenton 3 hourly diurnal mean air temperatures (solid, degrees Celsius) and station pressures (dashed lines, hPa) for the period 7 days before and after the ASTR (designated by the zero). The 7 day averages are shown as horizontal lines.

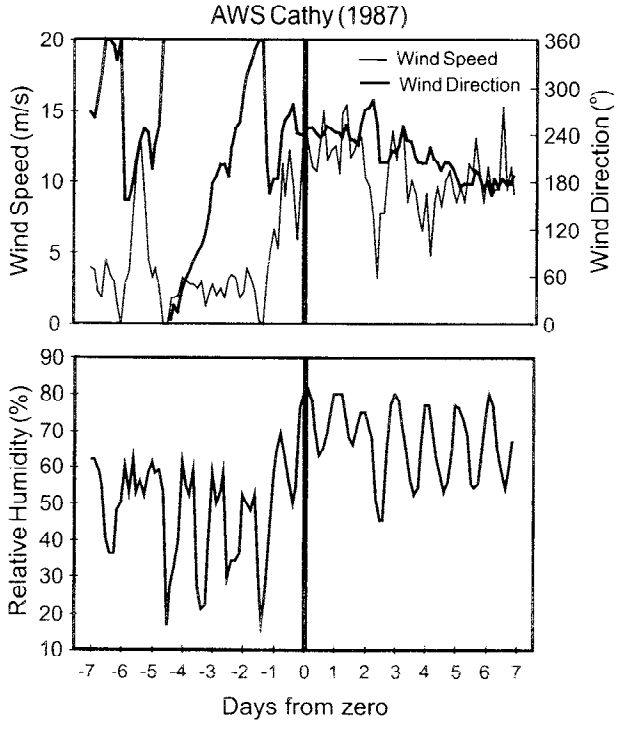

Figure 5. Mean daily wind direction, wind speed (meters per second) and relative humidity (percent) for AWS Cathy during the 7 days prior to and after the 1987 ASTR event.

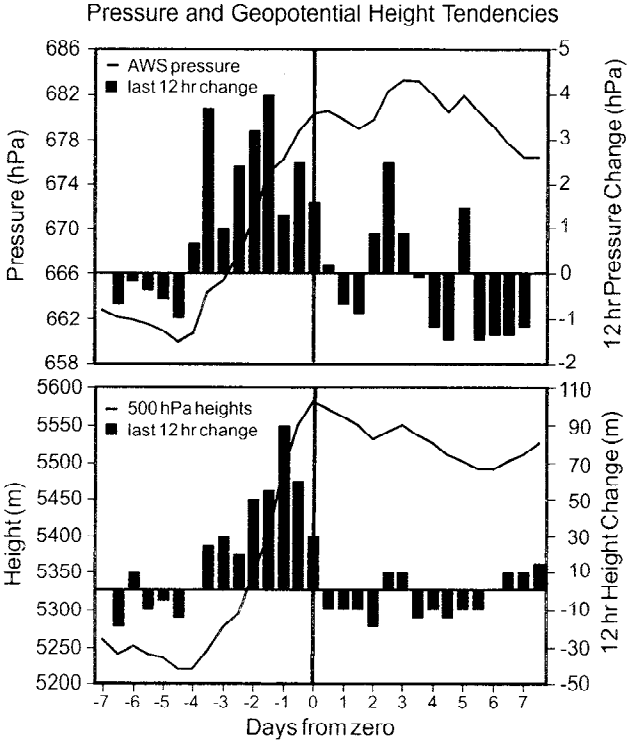

Figure 6. (Top) Composite-mean 12 hourly AWS pressures (thick line) and the 12-hour pressure tendencies (vertical bars) and (bottom) composite-mean 500 hPa heights (thin solid line) and 12-hour height tendencies (vertical bars) for the 7 day period before and after the abrupt spring air temperature rise on the Greenland ice cap.

after the event, although the range is reduced to about 5°C on T=0 and T+1.

As the composite ASTR consists of only six cases (years), it is affected by large interannual variations. For example, the small diurnal temperature range after day zero is especially apparent in 1987, 1992, and 1993, but the increase in the composite diurnal temperature on days T+3 and T+4 reflects extremely high air temperatures (+1.8°C on May 15, 1988 at 1800 UT: a data set record high). The extreme air temperatures may reflect a radiation error of the temperature sensor under conditions of high pressure and low wind (C.R. Stearns, personal communication, 1995). The diurnal range increase (Figure 4) also reflects a drop in 1992 air temperatures, nearly back to pre-ASTR levels on days T+3 to T+6, after which temperatures returned to higher values.

The AWS composite mean pressure reaches a minimum on T-5 and T-4 (Figure 4) and then steadily rises over 20 hPa to a double maximum around 680 hPa near T=0 and 682 hPa at T+3. The longer-term change in mean pressure (see Figure 2) is about 16 hPa (662 to 678 hPa). The double peak in the composite maxima in mean pressure at T=0 and T+3 reflect two specific events. In 1988, pressure rose about 40 hPa to 696 hPa between days T-3 and T+4, and in 1993 pressure rose over 45 hPa between days T-7 and T=0. Smaller pressure rises of 20-25 hPa, occurring over a period of 7 to 10 days, are apparent in 1987 and 1990; however, the 1992 event exhibited no consistent upward pressure trend. Details of the temperature and pressure records in each year are given by *Hellstrom* [1995].

In addition to cooling events that occur after somes ASTRs, such as that in 1992 (described above), abrupt warmings occasionally occur prior to the ASTR. Early warmings (e.g., in April 1989 [*Hellstrom*, 1995] and April and early May 1994) are characterized by pressure increases to approximately 685 hPa and air temperature maxima near -10°C. Although very much like the characteristic May ASTR events, both subsequently decline sharply. For example, in 1989 a long 4 week cold spell separates the early event from the ASTR event. The 1994 data show that air temperatures reached -10°C in late April and again on three occasions in May. The intervening cold spells last for a few days with temperatures decreasing to daily maxima between -15° to -20°C and minima near and below -30°C. We are inclined to believe that no clearly defined ASTR event occurs in 1994, in contrast to the preceding years.

ASTR events are accompanied by notable changes in wind speed and relative humidity, although only 1 year of data (1987) is available to support this suggestion. These data (Figure 5) indicate that mean winds increase from approximately 3 m s^{-1} prior to the ASTR to about 13 m s^{-1} after the event, afterward persisting at this velocity for 7 days. The wind direction was persistently from the southwest after the ASTR, with no calms. Morning relative humidities (Figure 5) increased from 60% prior to day zero to over 80% after the ASTR. Given an average station pressure of 680 hPa on the ice cap summit, the net change in maximum daily temperatures of 12°C due to the ASTR is linked to net changes in saturation mixing ratio (using standard meteorological tables) from 0.97 g kg^{-1} to 2.65 g kg^{-1}. The daytime relative humidities change (Figure 5) from about 25% to 50% (and higher on T=0 and T+1), thus suggesting that observed mixing ratios change from approximately 0.25 g kg^{-1} to 1.30 g kg^{-1}, indicating a sizable relative change in moisture flux across the ice cap summit with the 1987 ASTR.

The 12 hourly tendencies of pressure and 500 hPa height, obtained in the gridded data for 70°N, 40°W, show (Figure 6) that the largest mean pressure increases occur up to T=0 with comparatively small tendencies afterward to T+7. The 500 hPa mean geopotential height changes from 5220 m on day T-4 to 5580 m at T=0.

Atmospheric Circulation Variations Associated With the ASTR

Six year composite averages of sea level pressures (Figure 7) and 500 hPa heights (Figure 8) are illustrated twice prior to the ASTR, at T-6 and T-2 and on T=0 when the warming event has just occurred. The atmospheric circulation at T-6 represents conditions prevailing during the colder portion of the spring prior to any ASTR-related changes. The 500 hPa flow (Figure 8a) is characterized by a deep low

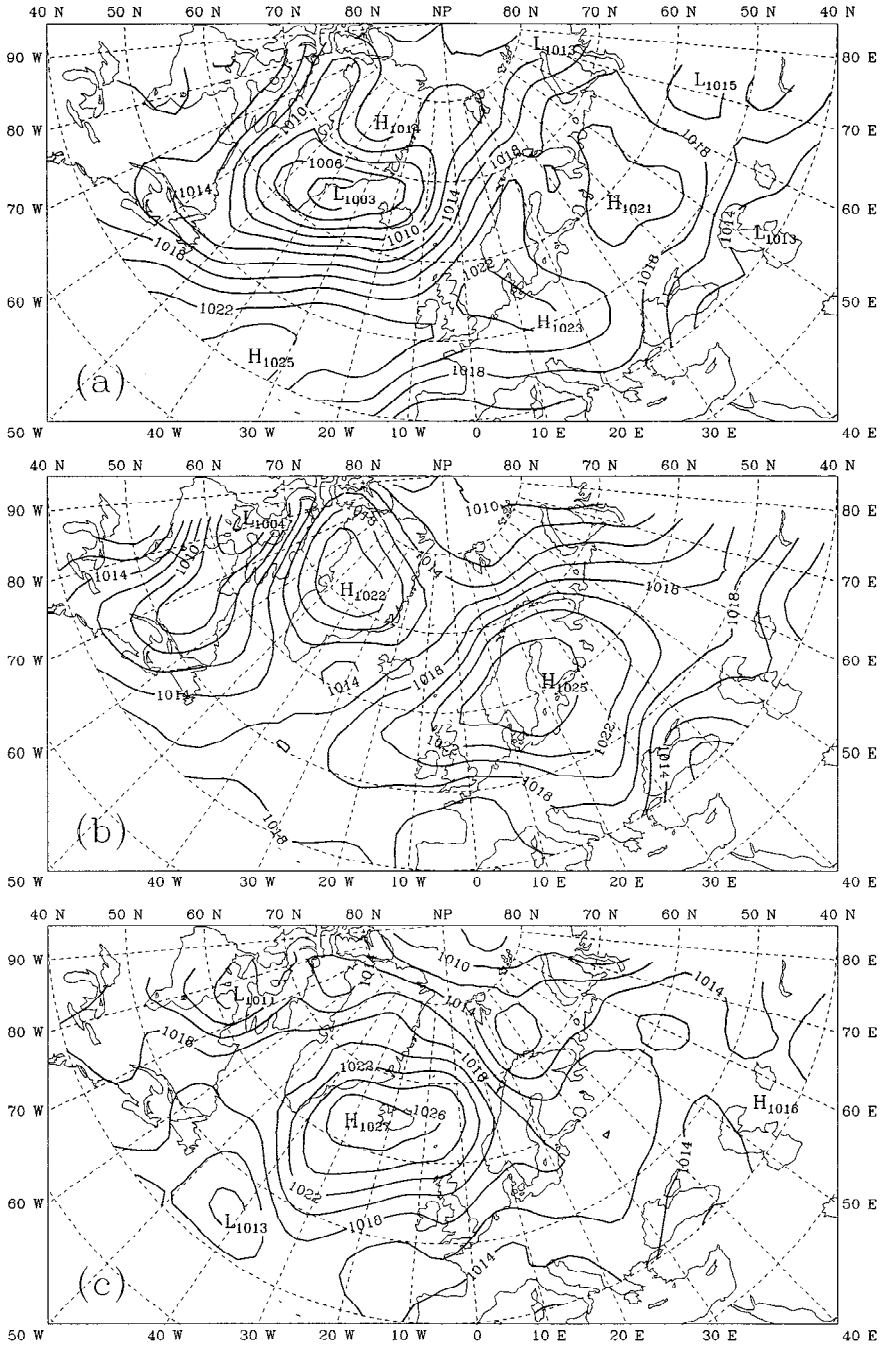

Figure 7. North Atlantic 6 year composite-mean sea level pressures occurring (a) six days prior, (b) two days prior, and (c) on the day of (day zero) the abrupt air temperature rise on the Greenland ice cap.

over Baffin Bay and a strong southwesterly flow over the northern Atlantic. A blocking ridge is beginning to build over central Europe and a separate northwest- to southeast-oriented ridge extends to northern Greenland. The ridge in central Europe persists and builds westward through the period and begins to amplify rapidly on T-3. The Icelandic low at sea level (Figure 7a) is deep (1003 hPa) and located in its long-term cold-season mean position over the Denmark Strait. It begins to weaken after T-4 as the upper level trough (Figure 8a) weakens over the Denmark Strait.

On T-2, high pressure is building over Greenland at both the surface (Figure 7b) and the 500 hPa level (Figure 8b). The short-wave ridge over Baffin Island and the Davis Strait (Figure 8b) has migrated into this position after passage and intensification across eastern Canada since T-4 (not shown), and it helps establish the positive height tendencies across the ice cap as shown in Figure 6b. The area of negative vorticity advection ahead of this Baffin ridge helps build the transient high-pressure cell over the ice cap (Figure 7b). Since T-4, this cell had also migrated across northeastern Canada and Baffin Island toward the ice cap.

The blocking anticyclone over western Europe and Scandinavia is a prominent feature of the regional circulation two days prior to the ASTR (Figure 7b and 8b). Another key feature of the upper air circulation is the ridge over the Atlantic, east of Newfoundland, with an axis along 45°W. This ridge subsequently remains quasi-stationary and on T-1 (not shown) sharply amplifies and builds toward the Denmark Strait. The circulation on T-1 thus exhibits blocking anticylones along both 45°W longitude as well as over western Europe, with an intervening cutoff trough between them in the central

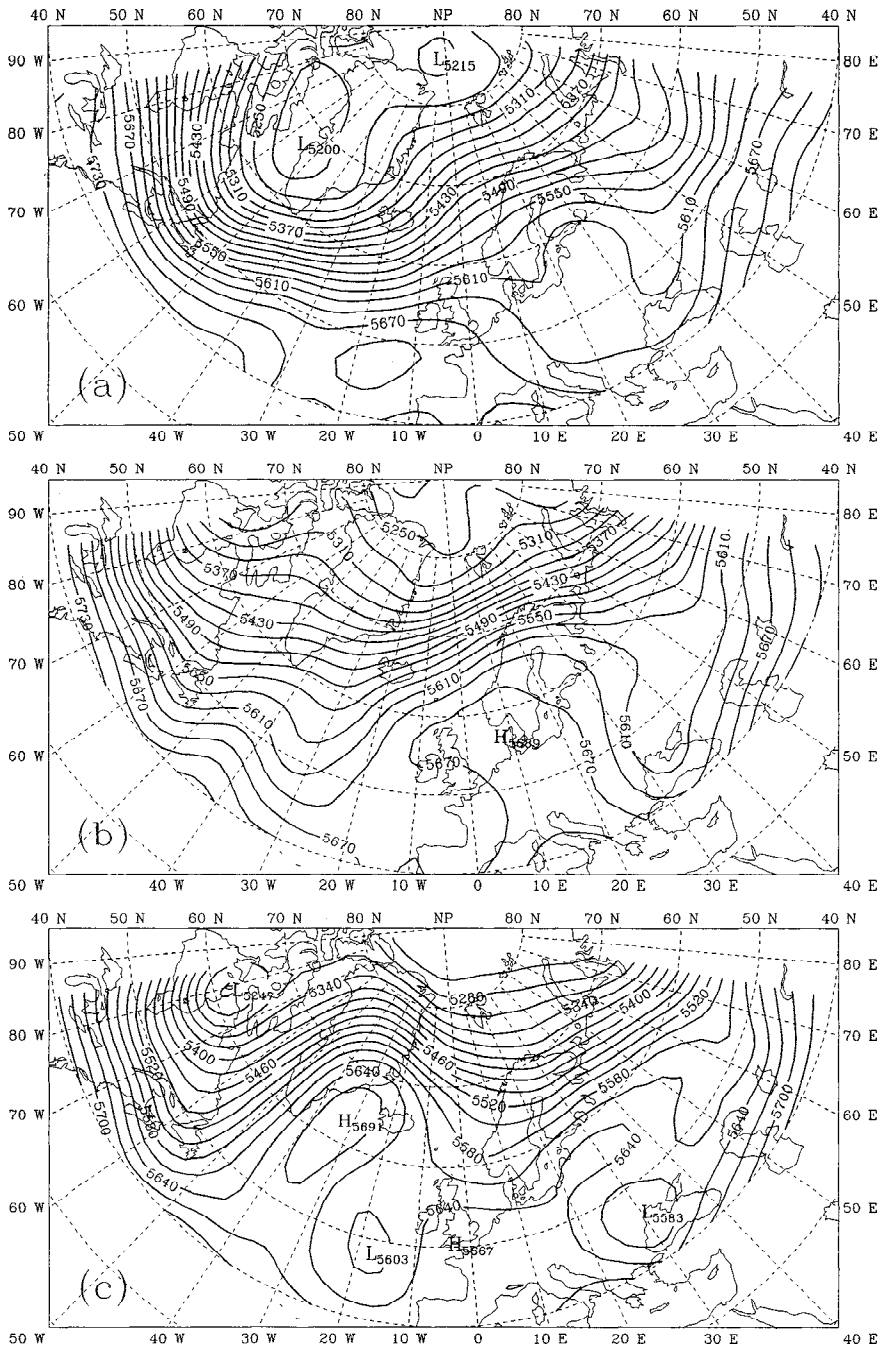

Figure 8. North Atlantic 6 year composite-mean 500 hPa geopotential heights occurring at (a) six days prior, (b) two days prior, and (c) on the day of (day zero) the abrupt air temperature rise on the Greenland ice cap.

Atlantic. A strong southerly flow begins to establish over the ice cap, while the Icelandic low (Figure 7b) dramatically weakens, and at T-2 becomes pinched between the surface high pressure cells over Greenland and Scandinavia.

At T=0 (Figures 7c and 8c) the abrupt warming is under way, and temperatures attain summertime levels. The 500 hPa blocking ridge over the Denmark Strait (Figure 8c) amplifies from its earlier position east of Newfoundland along 45°W on T-2 (Figure 8b), but the European ridge weakens as a trough passes across Scandinavia. The upstream Denmark Strait ridge has amplified since T-2 at the expense of the European ridge. The surface anticyclone over Iceland (Figure 7c) migrates into position from its earlier location (T-2) over Greenland (Figure 7b), and a sea level pressure of 1027 hPa occurs over the normal location of the Icelandic low. Over the prior 3 days the mean Denmark Strait pressure has increased by 20 hPa. The 500 hPa Denmark Strait blocking ridge (Figure 8c) is stacked over the surface high indicating establishment of a deep warm core blocking anticyclone. A strong pressure gradient and south-southwesterly flow is established over the ice cap. The westerlies are displaced into the high Arctic across the entire Atlantic-European sector. Although some variability occurs in the composite circulation patterns after T=0 (not shown, see *Hellstrom*, [1995]) the prevailing general anticyclonic nature of the circulation persists with high geopotential heights and southerly flow over the ice cap.

The annual course of monthly mean station sea level pressures at Ponta Delgada, Azores (38°N, 26°W), and Akureyri, Iceland (66°N, 18°W), is shown in Figure 9. The sea level pressures at these locations are representative of those for the mean Azores high and the

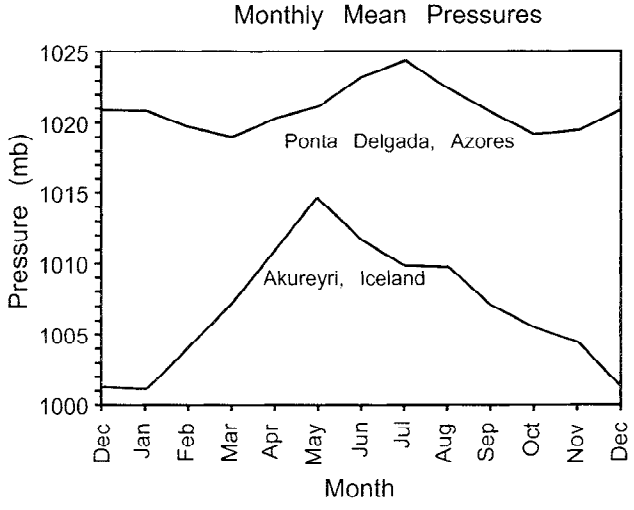

Figure 9. Monthly mean sea level pressures (hPa) at Akureyri, Iceland, and Ponta Delgada, Azores. Pressure differences between these stations are a measure of the strength of the Atlantic midlatitude westerlies.

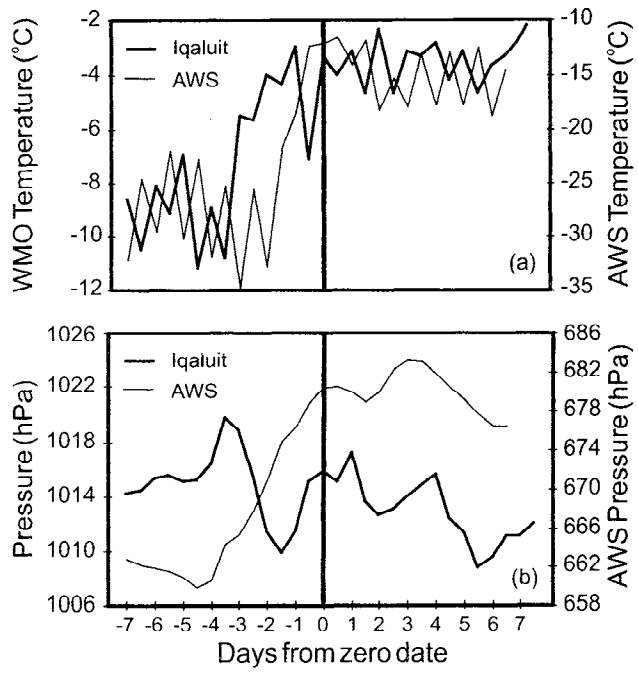

Figure 10. Six year composite (a) air temperatures (degrees Celsius) and (b) sea level pressures (hPa) for Iqaluit, Baffin Island (Figure 1) for 7 days prior to and after the ASTR on the Greenland ice cap (dashed lines). The composite AWS temperatures and pressures (solid lines) are shown for comparison.

Icelandic low pressure systems, and the gradient of pressure between them is a measure of the strength of the Atlantic midlatitude westerlies and of the North Atlantic Oscillation [*Rogers*, 1984]. In the annual cycle (Figure 9), sea level pressure over Iceland reaches a minimum in May, while pressure builds to a July maximum over the Azores. The pressure gradient and westerlies between the two locations are weakest in May and the mean pressure over Iceland remains high, near 1010 hPa, until August. The change in the atmospheric circulation between T-6 and T=0, leading to the ASTR, may be a regular climatological feature of the atmospheric circulation, producing the seasonal weakening of the westerlies in May. With the changes associated with the ASTR, a more meridional circulation regime occurs over the middle latitudes of the Atlantic, with blocking anticyclones at the surface and aloft, and the westerlies migrate northward over the higher latitudes. At sea level, the Icelandic low weakens substantially and is replaced by weak cyclonic activity or prevailing anticyclonic circulation.

The ASTR at Sea Level

The ASTR is also evident at some coastal meteorological stations (see Figure 1) lying near sea level on Baffin Bay, Greenland, and Iceland [*Hellstrom*, 1995]. At Iqaluit (see Figure 1), on southern Baffin Island, the composite air temperatures reveal an abrupt rise as early as T-3 (Figure 10a) with a net mean rise of about 7C° by T-1. The abrupt temperature rise coincides with a 678 hPa pressure maximum (Figure 10b) on T-4, after which, pressure decreases. Overall, the pressure variation pattern at Iqaluit is dissimilar to that occurring on the ice cap (Figure 10b) or at other nearby Greenland stations. Pond Inlet on northeastern Baffin Island (data not shown) only exhibits a slow rise in air temperature of about 8°C over the period T-5 to T+3.

The abrupt air temperature rise at Upernavik, Greenland, is characteristic (Figure 11a) of meteorological changes at Thule, Frederikshab, and even Danmarkshavn on northeastern Greenland (see Figure 1). However, the abrupt air temperature rise to T=0 is only about 6°C at Thule and Upernavik and 4°C at the southernmost (Frederikshab) and northeasternmost (Danmarkshavn) sites. Sea level pressure (Figure 11b) characteristically rises from 1006 hPa on T-6 to 1022 hPa on T-2, effectively preceding the ice cap changes by 1-2 days, although this is somewhat less apparent at Danmarkshavn (not shown). Comparatively, the sea level pressures (Figure 11b) decline more than those at the AWS after the primary pressure maximum at T+2.

A small composite temperature increase of about 2°C occurs at Kap Tobin (Figure 12a) during the week after the ice cap ASTR. This is representative of stations along the eastern coast of Greenland, including Angmagssalik, Prins Christian Sund, and at Iceland. These small temperature changes are not abrupt, but the sea level pressure signal (Figure 12b) at these stations is very pronounced. Sea level pressure rises from 1006 hPa to 1024 hPa over the period T-5 to T-1 (Figure 12b) with a secondary peak at T+3, very similar to the ice cap sea level pressure pattern.

In general, air temperature and sea level pressure variations at the coastal stations are consistent with those expected from the synoptic development illustrated in Figures 7 and 8. The early (T-3) temperature and pressure rise at Baffin Island (Figs. 10a and 10b) reflects the passage of the transient ridge across eastern Canada (see Figure 8b). Subsequently, the ridge passes over coastal stations on western Greenland, the ice cap, and then it merges with the blocking high over the Denmark Strait on day zero, when air temperatures have increased sharply on the ice cap. Western Greenland stations exhibit the pressure rise due to the transient ridge on day T-2 (see Figure 10b), but the temperature rise (Figure 10a) does not occur until day zero, as on the ice cap, when strong southwesterly flow is enhanced by the blocking ridge over the Denmark Strait. Although coastal air temperature changes are smaller than those over the ice cap, they are fairly abrupt over southern Baffin, on western Greenland and at Danmarkshavn, stations all located under the strong southerly flow on day zero (Figures 7c and 8c). The easternmost stations (Kap Tobin and Iceland) are not so affected by the strong thermal advection and exhibit little temperature change. However, it is apparent by comparing the sea level pressures over Iceland (Figures 7a and 7c) that these stations participate very strongly in the pressure field signal and are located at the core of some of the largest regional pressure changes.

Discussion

The atmospheric circulation changes associated with the ASTR (Figures 7 and 8) are consistent among the six years that comprise the composites, with the exception of 1992. The ASTR stands out clearly in the temperature time series for May 1992, but it is the smallest of the six events in terms of net temperature rise [*Hellstrom*, 1995]. It also occurs with only a small station pressure rise and there is a 4 day post-ASTR decline in air temperatures between T+3 and T+6. The

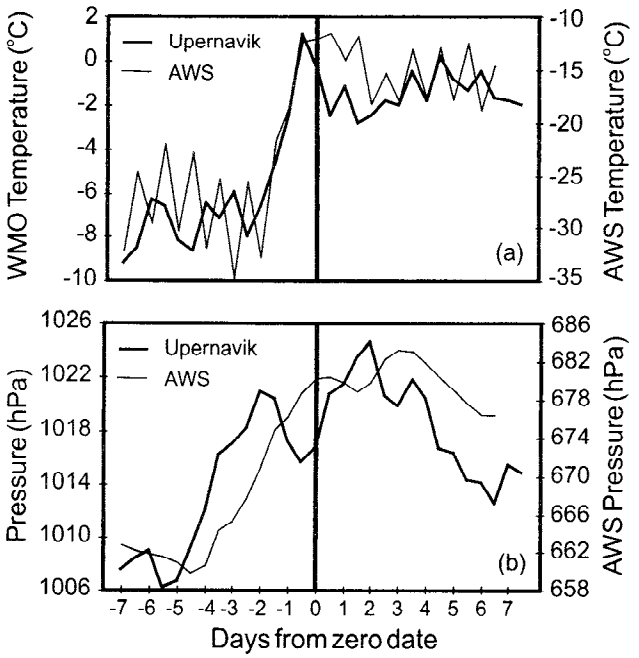

Figure 11. Same as Figure 10 but for Upernavik, Greenland (Figure 1).

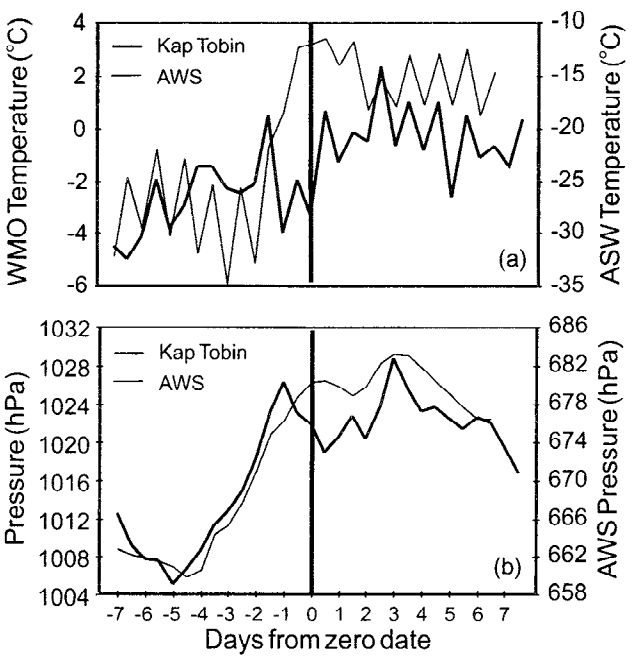

Figure 12. Same as Figure 10 but for Kap Tobin, Greenland (Figure 1).

1992 event is associated with a northwest-southeast 500 hPa ridge that extended from northern Greenland to southern Scandinavia and central Europe at T=0 [*Hellstrom*, 1995]. This is in contrast to the ASTRs of 1987, 1989, and 1990 which evolved due to the intensification of the northwestern Atlantic blocking ridge over the Denmark Strait (Figure 8c) and the ASTRs of 1988 and 1993 that are linked more to transient ridges that intensify and become quasi-stationary near southern Greenland. Overall, it appears that the ASTR is a manifestation of a seasonal atmospheric circulation change in which the westerlies and polar air are displaced northward and a persistent meridional flow regime becomes established in the North Atlantic. This is accompanied by the disappearance, or considerable weakening, of the Icelandic low. When this persistent regime fails to become established, the ASTR on the ice cap is less noticeable. For example, the early, or premature, ASTR events seem linked to transient synoptic systems that bring brief periods of high air temperature and pressure, followed by sharp declines in both. The large swings in air temperature in April and May 1994 are suggestive of numerous strong transient synoptic events.

In addition to regional atmospheric circulation variations the ASTR also appears associated with important changes in the atmospheric boundary layer and snow surface on the ice cap [*Hellstrom*, 1995]. The surface energy budget likely plays an important role, perhaps a decisive role, in maintaining ice cap air temperatures at summer levels after the ASTR. The early unsustained warming events observed in some years may occur because the surface energy budget is not yet able to maintain summer equilibrium conditions. The data presented here indicate that the ASTR is associated with (1) a decline in diurnal temperature range on T=0, T+1, and T+2; (2) increasing southwesterly surface flow accompanied by rising air temperatures; and (3) possibly increasing wind velocity and humidity. These changes are suggestive of increasing cloud cover as the ASTR occurs and of increasing strong advection of moisture and heat over the ice cap. These, in turn, suggest that substantial changes occur both in the radiation balance over the snow surface and in the surface boundary layer mixing. These factors may lead to changes in the snow surface, including some melting and surface albedo changes. In regions of little to weak katabatic flow, such as at the Greenland Summit, conditions in the post-ASTR period are favorable for summertime hoar frost formation [*Shuman et al.*, 1995b].

This examination of a limited number of abrupt springtime air temperature transitions over the Greenland ice cap may have implications for field studies. Scientific field work may be adversely affected in regions on the ice sheet where cloud cover and wind strength increase during ASTR events. People on the ice cap may not notice the air temperature rise during the ASTR due to the increased wind chill associated with increases in wind strength suggested in 1987 AWS data and by the strong pressure gradients over Greenland on T=0 (Figures 7 and 8). For example, the "wind chill" temperature is lower when air temperature is -10°C with a steady 13 m s^{-1} wind as compared to a situation prior to the ASTR with air temperatures of -22°C and only a 3 m s^{-1} wind. Ascertaining the relationships among clouds, near-surface wind speeds, surface air temperatures, the surface radiation budget, and boundary layer mixing over the ice cap may be resolved by future real-time observations such as might be made during a planned winter-over at the Second Greenland Ice Sheet Project (GISP II) (Summit) site.

The abrupt temperature transition over the ice cap may provide a physical basis for the fairly rapid change in $\delta^{18}O$ from winter to summer, which is most commonly used to separate winter and summer precipitation layers in ice core records. The reliability of ice core dating by $\delta^{18}O$ depends upon the strength of the expression of winter ($\approx$ -43‰) versus summer ($\approx$ -27‰) isotopic values [*Shuman et al.*, 1995b; *Bolzan and Stroebel*, 1994]. As more data become available, it may be possible to explore links between failure of the ASTR event and a reduced range in the winter to summer $\delta^{18}O$. Another possibility for future work is to characterize the strength of the blocking high (Figs. 7c and 8c) and to then examine the ice core $\delta^{18}O$ records from central Greenland for evidence of a "warm" isotopic spring/summer peak as would be expected with the intrusion of warmer, moist air from the south when the blocking high is well developed. It is likely that this circulation pattern would also be associated with an increase in the concentrations of atmospheric dust derived from eastern North America, and we are exploring Greenland ice core dust records for evidence of such intrusions. We plan to continue the synthesis of AWS data as they become available. With additional years of data it will be possible to confirm the reliability of the ASTR event and possibly isolate its occurrence and strength in ice core records.

Conclusions

We have described an abrupt springtime temperature rise (ASTR) that occurs over the Greenland ice cap and which is detected in the air temperature and pressure data from automatic weather stations. The ASTR typically occurs in May over a 24-36 hour period and is

accompanied by a large pressure rise beginning 2-3 days earlier. It is accompanied by an average rise of 360 m in the 500 hPa geopotential heights, strong ice cap surface winds, and high relative humidities. Concomitant air temperature changes at coastal weather stations on western Greenland are only half the magnitude of those occurring on the ice cap summit, but the ASTR pressure rise at coastal stations around Greenland and Iceland is of equivalent magnitude to that at the summit. We show that the ASTR is linked to a seasonal weakening of the midlatitude westerlies that culminates in the month of May and persists through summer. A meridional flow regime is established over the northern Atlantic with blocking highs at the surface and aloft. The surface mean Icelandic low weakens or is replaced by relatively high pressure over the Denmark Strait. An awareness of the ASTR is important for planning springtime field activities on the Greenland ice sheet. Further study of the ASTR should lead to a better understanding of boundary layer processes over the ice sheet and should help determine whether the ASTR leaves a discernible chemical or physical signal in the stratigraphy of the ice sheet.

Acknowledgments. This work is supported by the NOAA Office of Global Programs-Atlantic Climate Change Program under grants NA36GP0236 and NA56GP0213. John Nagy and Jeannie Jaros, of the Byrd Polar Research Center, assisted in producing the diagrams. This is Byrd Polar Research Center contribution 997.

References

Bolzan, J.F., and M. Strobel, Accumulation-rate variations around Summit, Greenland, *J. Glaciol., 40*(134), 56-66, 1994.

Bromwich, D.H., and C.R. Stearns (Eds.), *Antarctic Meteorology and Climatology: Studies Based on Automatic Weather Stations*, Antarct. Res. Ser., vol. 61, 207pp., AGU, Washington, D. C., 1993.

Hellstrom, R.A., The abrupt spring temperature rise and pressure increase over the Greenland ice sheet, 154 pp., Atmospheric Sciences Program, M.S. thesis, Ohio State Univ., Columbus, 1995.

Rogers, J.C., The association between the North Atlantic Oscillation and the Southern Oscillation in the Northern Hemisphere, *Mon. Weather Rev., 12*, 1999-2015, 1984.

Shuman, C.A., R.B. Alley, S. Anandakrishnan, and C.R. Stearns, An empirical technique for estimating near-surface air temperature trends in central Greenland from SSM/I brightness temperatures, *Remote Sens. Environ., 51*(2), 245-252, 1995a.

Shuman, C.A., R.B. Alley, S. Anandakrishnan, J.W.C. White, P.M. Grootes, and C.R. Stearns, Temperature and accumulation at the Greenland Summit: Comparison of high-resolution isotope profiles and satellite passive microwave brightness temperature trends, *J. Geophys. Res., 100*, 9165-9177, 1995b.

Stearns, C.R., and G.A. Weidner, Snow temperature profiles and heat fluxes measured on the Greenland crest by an automatic weather station, in International Conference on the Role of the Polar Regions in Global Change edited by G. Weller, pp. 223-226, Univ. of Alaska, Fairbanks, 223-226, 1991a.

Stearns, C.R., and G.A. Weidner, The Polar Automatic Weather Station Project of the University of Wisconsin, in International Conference on the Role of the Polar Regions in Global Change, edited by G. Weller, pp. 58-62, Univ. of Alaska, Fairbanks, 1991b.

Jeffrey C. Rogers, Department of Geography, 1036 Derby Hall, 154 North Oval Mall, The Ohio State University, Columbus, OH, 43210-1361 (e-mail:jcrogers@geography.ohio-state.edu)

Robert A. Hellstrom, Atmospheric Sciences Program, 1036 Derby Hall, 154 North Oval Mall, Columbus, OH, 43210-1361 (e-mail: rhellstr@magnus.acs.ohio-state.edu)

Ellen Mosley-Thompson, Byrd Polar Research Center, 108 Scott Hall, 1090 Carmack Road, The Ohio State University, Columbus, OH 43210 (e-mail:thompson.4@osu.edu)

Chung-Chieh Wang, Atmospheric Sciences Program, 1036 Derby Hall, 154 North Oval Mall, Columbus, OH 43210-1361 (e-mail: cwang@geography.ohio-state.edu)

(Received December 20, 1995; revised July 12, 1996;
accepted September 1, 1996)